Histol Histopathol (2019) 34: 765-774

http://www.hh.um.es

Histology and Histopathology

From Cell Biology to Tissue Engineering

Reduction of PGRN increased fibrosis during skin wound healing in mice

Shan-shan Li[1]*, Mei-xiang Zhang[1]*, Yue Wang[1], Wei Wang[1], Chun-ming Zhao[2], Xiao-ming Sun[1], Guo-kai Dong[1], Zhou-ru Li[1], Wen-jiang Yin[1], Bo Zhu[3] and Hong-xing Cai[1]

[1]Department of Forensic Medicine, [2]Department of Human Anatomy, Xuzhou Medical University, Xuzhou, Jiangsu, P.R. China and [3]Department of Pharmacology and Experimental Therapeutics, Boston University School of Medicine, Boston, Massachusetts, USA

*These authors contributed equally to this work

Summary. Progranulin (PGRN) is a multi-functional growth factor known to be involved in regulating of development, cell cycle progression, cell motility, tumorigenesis and angiogenesis. Research has revealed that PGRN is a crucial mediator of skin wound healing. Nonetheless, the role of PGRN in the fibrosis process of cutaneous wound healing has not been identified. In the present study, mice with excisional wounds were treated with si-m-PGRN or physiological saline. We observed the expression of PGRN in intact and post-injury skin by immunohistochemistry. Tissue sections of skin around the wound were performed by hematoxylin and eosin and masson's trichrome staining. After PGRN knockdown by siRNA, the expression of PGRN, collagen I (Col I), small mothers against decapentaplegic homolog 3 (Smad3), phosphorylated Smad3 (P-Smad3), transforming growth factor (TGF)-β1 and TGF-β receptor I (TβRI) were detected by real-time reverse transcription polymerase chain reaction (RT-qPCR) or Western blot. PGRN mRNA and protein expressions were increased after insult and remained above that of intact skin through day 20. Down-regulation of PGRN augmented fibrosis area, skin thickness and the expression of Col I. In addition, reduction of PGRN considerably increased the expression of TGF-β1, TβRI, Smad3 and P-Smad3. These results indicate that PGRN knockdown enhances the fibrosis degree, probably via the TGF-β/Smad signaling pathway.

Key words: Cutaneous wound healing, Fibrosis, PGRN, TGF-β/Smad

Offprint requests to: Professor Hongxing Cai, Deparment of Forensic Medicine, Xuzhou Medical University, 84 Western Huaihai Road, Xuzhou, Jiangsu 221000, P.R. China. e-mail: xzykdxchx@163.com

DOI: 10.14670/HH-18-076

Introduction

Cutaneous wound healing is one of the most complex processes in containing overlapping phases, hemostasis/ inflammation phase, proliferation phase and remodeling phase. Many types of cell, including immune cells (neutrophils, monocytes, lymphocytes and dendritic cells), endothelial cells, keratinocytes and fibroblasts, undergo marked changes in gene expression and phenotype, leading to cell proliferation, differentiation and migration during wound healing. The outcome is generally imperfect, with some degree of fibrosis or scarring, which is defined by the accumulation of excess extracellular matrix components. If highly progressive, the fibrotic process eventually leads to organ malfunction, which will become even more burdensome in both human health and economic terms (Gurtner et al., 2008; Eming et al., 2017; Kiritsi and Nyström, 2018). Hence, it is needed to further unveil the mechanism of wound healing and find more effective therapy targets of extra fibrosis.

Many kinds of cytokines and growth factors, such as progranulin (PGRN), participate in the wound healing process. PGRN, also called granulin or epithelin

precursor, acrogranin or PC-derived growth factor, is a growth factor involved in tumorigenesis and development. Wounding induces PGRN gene expression in dermal fibroblasts, endothelial cells and infiltrating leukocytes (He et al., 2003). These led to suggestions that PGRN gene products are involved in the wound response. Nevertheless, the impact of PGRN on the fibrotic responses remains poorly understood. In this study, we propose a role for PGRN in the fibrosis process of skin wound healing.

Materials and methods

Animals and experimental protocol

A total of 33 male, wild-type BALB/c mice (6 weeks old; 20±3 g) were housed individually and acclimated to their environment for at least 1 week prior to surgery, in a temperature-controlled animal facility with a 12h light/dark cycle and *ad libitum* access to water and chow. The present study was approved by the Ethics Committee of Xuzhou Medical University (Xuzhou Jiangsu, China). Excisional wounds were performed on mice as described previously (Li et al., 2016; Wang et al., 2016). Briefly, following intraperitoneal injection with 1% sodium pentobarbital (40 mg/Kg), hair cutting and sterilization, we used 3M transparent ventilation tape splinting tightly adhered around the skin to be excised. Two full thickness (penetrating the tape and skin) circular punch wounds (4 mm diameter) were created symmetrically over the midline of the mouse dorsum. Thus, the inner edge of the tape exactly matched the edge of the wound; the tape adhered to the skin tightly and prevented contraction. Postoperatively, the mice were housed individually to minimize wound disruption, with access to food and water ad libitum (Fig. 1A). After surgery, the mice were randomly assigned into two groups and subjected to subcutaneous injection every four days with si-m-PGRN (2OMe+5Chol) (2.5 nmol dissolved in 30 µl physiological saline) synthesized by Guangzhou RiboBio Co., Ltd. (cat. no. siM170331023550, Guangzhou, China) or physiological saline (30 µl). Mice from each group were sacrificed by intraperitoneal injection with an overdose of sodium pentobarbital on days 4, 8, 12, 16 and 20 after surgery (3 mice at each time point).

Tissue preparation and histological analysis

Skin tissues were immediately fixed in 4% paraformaldehyde (Sinopharm Chemical Reagent Co., Ltd, Shanghai, China) with phosphate-buffered saline (pH 7.4) and embedded in paraffin according to the standard procedure. Specimens were then cut into 5 µm-thick sections and stained using hematoxylin and eosin (hematoxylin, Fluka, California, USA; eosin, Shanghai Zhanyun Chemical Co. Ltd, Shanghai, China) and Masson's trichrome staining (Ponceau Acid Acid Magenta Dye, Beijing Lengene Biotechnology Co., Ltd, Beijing, China; Phosphomolybdic acid aqueous solution, Beijing Lengene Biotechnology Co., Ltd; Light Green SF Yellowish Stain Solution, 1%W/V, Solarbio Life Sciences). Skin thickness was evaluated under VS120 Virtual Slide Microscope (x40; Olympus VS120; Digital slide scanning system; Beijing, China) by measuring the distance between the epidermis and the dermal-subcutaneous fat junction, in five randomly selected fields for each skin section. Correspondingly, fibrosis area and the number of fibroblasts were calculated by Image-Pro Plus 6.0 software.

Immunohistochemistry

Immunohistochemical staining was performed on 5 μm sections using the Universal Two-step kit (cat. no. PV-9000; Zsbio Commerce Store, Inc; Beijing, China) to evaluate the expression levels of anti-Granulin (rabbit polyclonal antibody; cat. no. ab92486; Abcam, Cambridge, UK; 1:200 dilution) according to the manufacturer's protocol. The positive cells were visualized using diaminobenzidine (cat. no. ZLI-9018; Zsbio Commerce Store). As immunohistochemical control for the immunostaining procedure, additional sections were incubated with phosphate-buffered saline (pH 7.4) in place of the primary antibody.

RNA isolation and RT-qPCR

Total RNA was isolated from the skin specimen (100 mg each) and extracted with TRIzol® Reagent (cat. no. 15596-018; Thermo Fisher Scientific, Inc., Waltham, MA, USA) following the manufacturer's instructions. Briefly, skin specimens were chopped and ground with glass homogenizer on ice, and then mixed with 1 ml TRIzol solution for 30 min at room temperature. The solution was centrifuged at 12,000×g for 15 min at 4°C, and the resulting supernatant was obtained. Following mixing with 200 μl chloroform (Sinopharm Chemical Reagent Co., Ltd), the solution was centrifuged again as before and then the resulting supernatant supplemented with equal volume isopropanol (Macklin). Following further centrifugation as before, the precipitate was collected and washed with 75% ethanol (Shanghai Lingfeng Chemical Reagent Co., Ltd), centrifugation as before, then repeated. The RNA pellet was air-dried and dissolved in 60 μl DEPC (Solarbio). RNA was reverse-transcribed using a High-Capacity cDNA Reverse Transcription kit (cat. no. 4368814; Thermo Fisher Scientific, Inc.). The obtained cDNA was then amplified by the ABI 7500 Real-Time PCR system (Applied Biosystems; Thermo Fisher Scientific, Inc.) using a PowerUp™ SYBR™ Green Master Mix (cat. no. A25742; Thermo Fisher Scientific, Inc.). The 10 µl reaction system contained the following: 5 µl PowerUp™ SYBR™ Green Master Mix (2X), 2 µl Nuclease-Free Water, 1 µl PCR forward primer, 1 µl PCR reverse primer and 1 µl cDNA. The qPCR reaction

was performed in the thermal cycler using the following conditions. Amplification was followed by 2 min at 50°C, 2 min at 95°C, and 40 cycles of 15 sec at 95°C, 15 sec at 57°C, 1 min at 72°C min and one cycle of 95°C for 15 sec, 60°C for 1 min and 95°C for 15 sec for fluorescence signal acquisition. Primer sequences were designed using Primer-BLAST and were synthesized by Genscript, Inc. (Table 1). The results were normalized against the expression level of β-actin. DdH2O was used instead of cDNA as negative control. Relative quantification was performed using the comparative quantification cycle (ΔΔCQ) method.

Protein preparation and immunoblotting assay

After chopping and grinding with glass homogenizer on ice, skin sample was mixed with pre-cooled 1 mL of RIPA lysis buffer (cat. no. P0013B; Beyotime Institute of Biotechnology; Shanghai, China), 10 μL of PMSF (cat. no. ST506; Beyotime Institute of Biotechnology) and 10 μL of phosphatase inhibitor (cat. no. KGP602; KeyGEN BioTECH; Jiangsu, China). The homogenate was centrifuged two times at 12,000×g for 15 min at 4°C, and the resulting supernatant was collected. Protein concentrations were determined, according to the manufacturer's protocol, with the enhanced BCA Protein Assay Kit cat. no. P0010; Beyotime Institute of Biotechnology). Subsequently, 30 μg of total protein was separated on 10% polyacrylamide gels (cat. no. P0012A; Beyotime Institute of Biotechnology) and transferred onto polyvinylidene fluoride membranes (EMD Millipore, Billerica, MA, USA) for 100 V for 1 h at room temperature. The membranes were blocked with 5% nonfat milk in Tris-buffered saline containing 0.1% Tween-20 (TBST; cat. no. 20170515; Shanghai Lingfeng Chemical Reagent Co., Ltd; Shanghai, China) at room temperature for 2 h and were then incubated overnight at 4°C with primary antibodies. The specifications and dilutions for the primary antibodies were as follows: Rabbit anti-Granulin polyclonal antibody (cat. no. ab92486; Abcam; 1:1000 dilution); rabbit anti-TβRI polyclonal antibody (cat. no. ab31013; Abcam; 1:500 dilution); mouse anti-TGF-β1 monoclonal antibody (cat. no. sc-130348; Santa Cruz Biotechnology, Inc.; Dallas, Texas, USA; 1:100 dilution); mouse anti-Smad3(38-Q) monoclonal antibody (cat. no. sc-101154; Santa Cruz Biotechnology, Inc;1:200 dilution); mouse anti-COL1A2(E-6) monoclonal antibody (cat. no. sc-393573; Santa Cruz Biotechnology, Inc. 1:100 dilution); rabbit anti-Smad3 (Phospho-Ser425) polyclonal antibody (cat. no. D155153; Sangon Biotech (Shanghai) Co., Ltd; Shanghai, China; 1:500 dilution). Mouse anti-GAPDH monoclonal antibody (cat. no.60004-1-Ig; Proteintech Group, Inc.; CHI, Illinois, USA; 1:6000 dilution) was used as a loading control. Following rinsing with TBST, the membranes were incubated with polyclonal goat anti-rabbit (cat. no. D110058; BBI Life Science) or anti-mouse (cat. no.VA002; VICMED Life Sciences, Inc.; Xuzhou, Jiangsu, China; both 1:5,000 dilution) secondary antibodies for 2 h at room temperature. The membranes were washed again with TBST and developed using a PierceTM ECL Western Blotting Substrate (cat. no. 32106; Thermo SCIENTIFIC) following the manufacturer's protocol. The bands of the blot were quantified by densitometry using Image J software (Image J 1.48 v; National Institutes of Health, Bethesda, MA, USA).

Statistical analysis

SPSS for Windows 16.0 was used for all statistical tests and calculations. Differences between vehicle group and si-m-PGRN group were assessed using Student's t test. One-way ANOVA analysis followed by Dunnett (the variance was homogeneous) or Dunnett's T3 (the variance was heterogeneous) *post hoc* test was adopted to determine the significant differences between control group and vehicle group. All data were presented as the mean ± standard deviation. Values of $P<0.05$ were considered statistically significant.

Results

PGRN expression in cutaneous wound healing

To investigate the effect of PGRN on fibrosis during skin wound healing, excisional wounds were performed on mice as described previously (Fig. 1A) (Li et al., 2016; Wang et al., 2016). We detected PGRN expression by immunohistochemistry staining for intact skin and wounded tissues of adult mice 4, 8, 12, 16 and 20 days after transcutaneous punch biopsy wounds. Fibroblasts and epithelial cells did not express PGRN in intact skin (Fig. 1B). On day 4 after surgery, mononuclear cells (MNCs) and spindle-shaped fibroblast cells (FBCs) expressed PGRN (Fig. 1C). On day 8 after surgery, FBCs became the main component of the wound generally, which also expressed PGRN (Fig. 1D). Not only that, we also observed PGRN in vascular endothelial cells (Fig. 1E). Intriguingly, epithelial cells did not express PGRN in intact skin but expressed after

Table 1. Sequences of the primers used for reverse transcription-quantitative polymerase chain reaction analysis.

Gene	Primer	Sequence (5'-3')
β-actin	forward	ACCTTCTACAATGAGCTGCG
	reverse	CTGGATGGCTACGTACATGG
Col I	forward	CATAAAGGGTCATCGTGGCT
	reverse	TTGAGTCCGTCTTTGCCAG
Granulin	forward	CACCTGCTGCATTATGGTTG
	reverse	CATCGTGTGTGAACCAGGTC
TGF-β1	forward	CCTGAGTGGCTGTCTTTTGA
	reverse	CGTGGAGTTTGTTATCTTTGCTG
Smad3	forward	GTGCGAGAAGGCGGTCAAGAG
	reverse	CCACAGGCGGCAGTAGATAACG

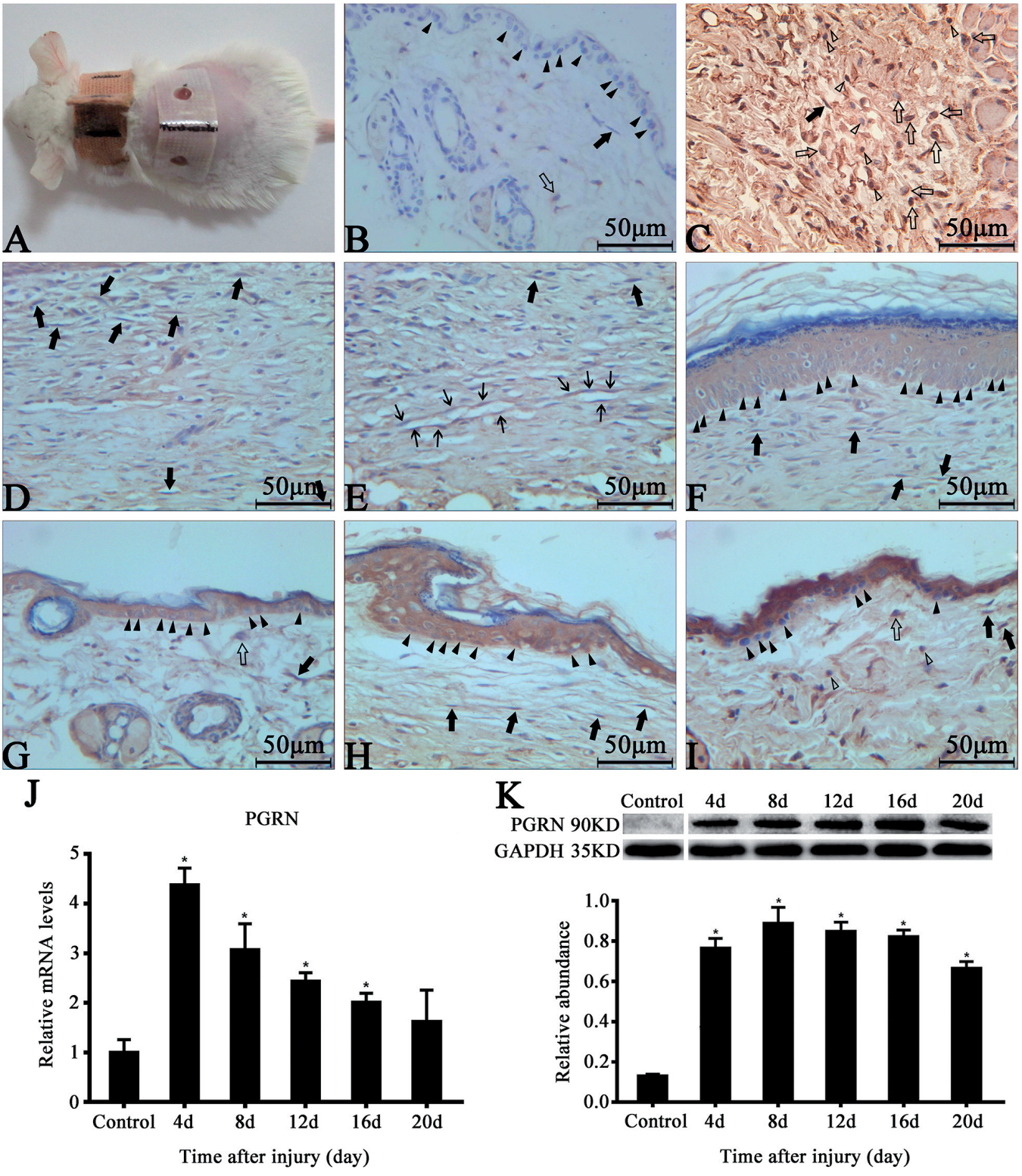

Fig. 1. PGRN expression in cutaneous wound healing. **A.** 4-mm punch wounds were performed on the dorsal side of splinting model mice. **B-I.** Representative immunohistochemical staining for PGRN was shown for different time points in the vehicle group. **B.** Intact mouse skin. The area of the wound at 4 d **(C)**, 8 d **(D)** and **(E)**, 12 d **(F)**, 12 d **(G)**, and 20 d **(H)**. **I.** The area around the wound at 20 d. **J.** PGRN mRNA expression levels in the vehicle group and the control group were analyzed by RT-qPCR and normalized to β-actin. **K.** Representative Western blot analysis for PGRN in the vehicle group and the control group. Epithelial cells are indicated by filled triangle, fibroblasts are indicated by filled arrow, macrophages are indicated by hollow arrow, mononuclear cells are indicated by hollow triangle, endothelial cells are indicated by thin arrow. All values are expressed as the mean ± standard deviation (n=5). *P<0.05, compared with the control group. Scale bars: 50 μm.

insult, and some of them, in the vicinity of the wound, did not express PGRN at later stages of the wound healing (Fig.1B,F-I).

We also detected PGRN mRNA by RT-qPCR analysis and protein by western blot in wound tissues. The mRNA and protein levels of PGRN increased after

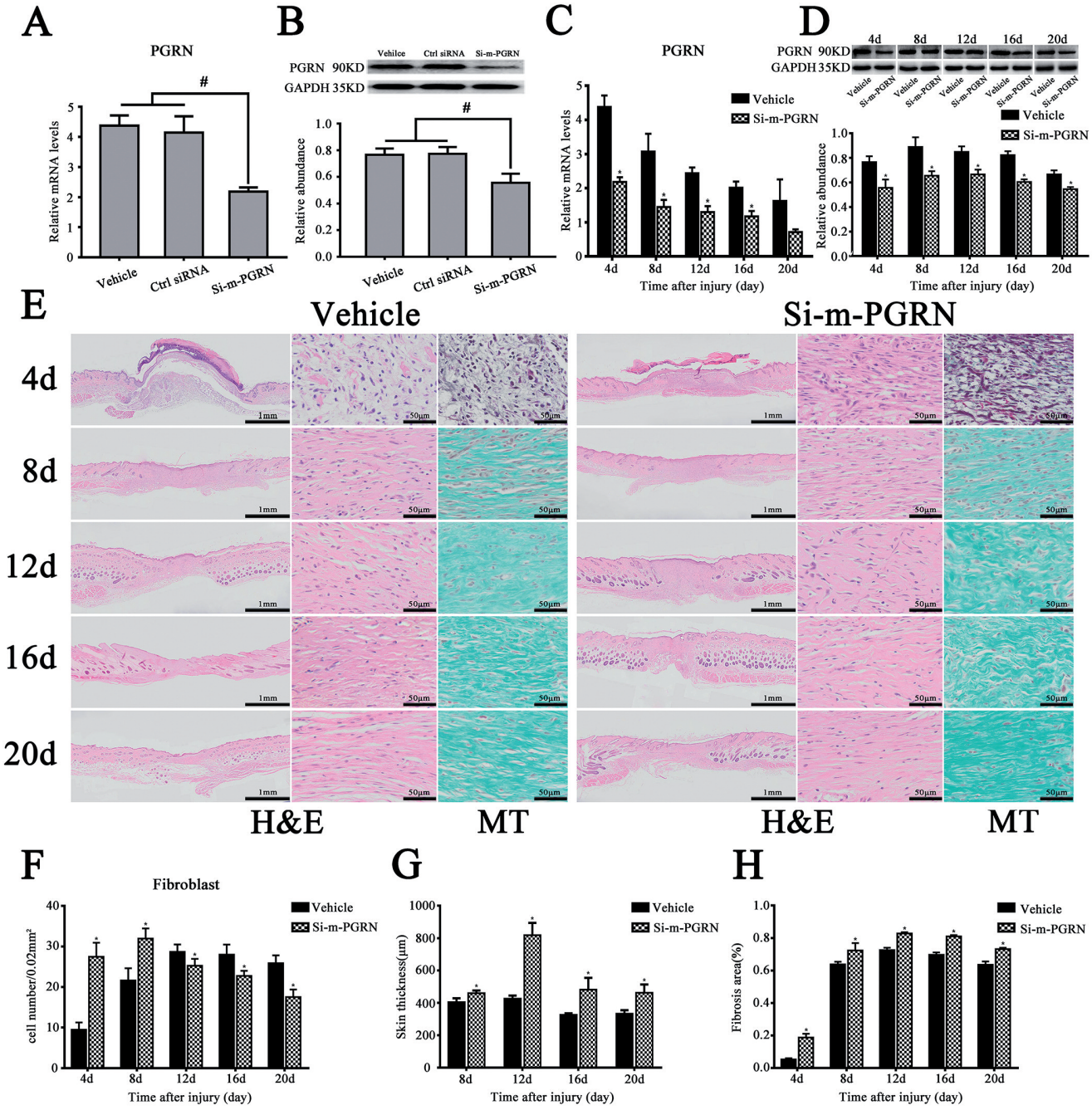

Fig. 2. Reduction of PGRN increased fibrosis. **A, B.** The mRNA and protein expressions of PGRN in the vehicle group, ctrl siRNA group and si-m-PGRN group. **C.** The effects of si-m-PGRN on PGRN mRNA expression levels in the vehicle group and the si-m-PGRN group were analyzed by RT-qPCR and normalized to β-actin. **D.** Representative Western blot analysis for PGRN protein levels in the vehicle group and the si-m-PGRN group. **E.** Pictures of H&E and Masson's trichrome (MT) stained sections of vehicle or si-m-PGRN treated wounds on different point during wound healing. **F.** Cell numbers of fibroblasts in the wounds at 4, 8, 12, 16, and 20 days post injury. **G.** Skin thickness at 8, 12, 16, and 20 days post injury. **H.** Quantitative summary of fibrosis area by Masson's trichrome staining. All values are expressed as the mean ± standard deviation (n=5). #P<0.05, compared with the vehicle group and the ctrl siRNA group. *P<0.05, compared with the control group.

injury (Fig. 1J,K, P<0.05) and remained above that of intact skin through 20 days after injury, indicating a role for PGRN in the wound response.

Reduction of PGRN increased fibrosis

We tested the transfection effect by using the 4-day samples administrated with si-m-PGRN, mismatched-siRNA or saline, and found that the mRNA and protein expressions of PGRN in saline and mismatched-siRNA group had no significant differences (Fig. 2A,B, P<0.05). Hence, we used saline as control in subsequent analysis. Then we treated mice with si-m-PGRN or physiological saline to test whether the si-m-PGRN could reduce the expression of PGRN. Data showed that the mRNA and protein levels of PGRN in si-m-PGRN treated group were significantly lower than that in vehicle group (Fig. 2C,D, P<0.05). Thus, we used the si-m-PGRN testing the effect of PGRN on fibrosis of wound healing. We performed H&E and masson's trichrome staining on tissue sections of 4th, 8th, 12th, 16th and 20th days after surgery (Fig. 2E). We found that MNCs and FBCs, which were identified by their morphological characteristics on H&E stained slices and the immunohistochemistry stains (data not shown), infiltrated in the wounded zone at 4 days post-injury. In the vehicle group, the number of FBCs increased after insult and reached a peak at day 12 post-injury. However, the number of FBCs was rapidly increased and peaked at day 8 after PGRN knockdown (Fig. 2F, P<0.05). Degree of fibrosis was evaluated by measuring the skin thickness and fibrosis area. The results revealed that the skin thickness and fibrosis area attained the peak at 12 days after injury. The si-m-PGRN group illustrated increased skin thickness and fibrosis area compared with the vehicle group (Fig. 2G,H, P<0.05).

As shown in Fig. 3A,B, the mRNA and protein levels of Col I snowballed during the cutaneous wound healing. After PGRN knockdown, the expression of Col I increased markedly compared with the vehicle group (Fig. 3C,D, P<0.05). These results suggested that the reduction of PGRN promoted fibrotic progress.

Effects of PGRN on TGF-β/Smad signaling pathway

To evaluate the effects of PGRN on the TGF-β/Smad signaling, we performed RT-qPCR and western blot to detect the mRNA and protein expressions of TGF-β1, Smad3 etc. The results revealed that the mRNA expression of TGF-β1 increased after insult and reached a peak at day 8 post-injury (Fig. 4A, P<0.05). The protein expression of TGF-β1 was down-regulated markedly at day 4 and increased gradually at day 8 and 12, and then gradually subsided at 16 and 20 days post-injury (Fig. 4B, P<0.05). The si-m-PGRN group had higher TGF-β1 expression compared with the vehicle group. Reduction of PGRN significantly heightened gene expression of TGF-β1 (Fig. 4C, P<0.05). The protein levels of TGF-β1 in the si-m-PGRN group were considerably increased compared with those in the vehicle group (Fig. 4D, P<0.05). The expression of TβRI, which was similar to the protein levels of TGF-β1, declined at day 4 after injury and then increased gently (Fig. 4E, P<0.05). At day 4, 8 and 12, the expression of TβRI in the si-m-PGRN group was significantly higher, compared with those in the vehicle group (Fig. 4F, P<0.05).

The expression of Smad proteins, which are the downstream mediators of canonical TGF-β signaling, had also been affected. The mRNA expression of Smad3 was up-regulated slowly and reached a peak at 8 days and reduced gradually at 12 days post-injury (Fig. 4G, P<0.05). At the same time, protein expressions of Smad3 and P-Smad3 gradually decreased after injury, rapidly increased and peaked at day 12, and then moderately diminished (Fig. 4H, P<0.05). Additionally, there was a marked upregulation of Smad3 in the si-m-PGRN group at 8, 12 and 16 days, and no changes were detected on day 4 and 20, compared with the vehicle group (Fig. 4I,J, P<0.05). Significant differences in P-Smad3 were detected between the si-m-PGRN and vehicle group at 4, 8, 12 and 16 days post-traumatic interval (Fig. 4J, P<0.05).

Discussion

In the present study, we found that PGRN plays an important role mediating fibrosis process of skin wound healing, as evidenced by the aggravation of fibrosis after PGRN knockdown, which may be via the TGF-β1/Smad3 signaling pathway. The paucity of data regarding the relationship between PGRN and fibrosis in skin wound healing notwithstanding PGRN is a multi-functional growth factor.

Skin wound healing is a continuous and complex biological phenomenon that is influenced by various internal and external factors and overlap in time and space. The process of wound healing can be divided into three sequential phases, inflammatory phase, proliferative phase and remodeling phase (Seo et al., 2017). Unbalance of one or more of these phases may have two distinct damaging consequences: the development of a chronic wound or the formation of a hypertrophic scar/keloid (He et al., 2003; Eming et al., 2017; Kiritsi and Nyström, 2018). Injury induced expression of numerous cytokines in various cell types must be activated and coordinated if tissue integrity and homeostasis are to be restored (Gurtner et al., 2008; Eming et al., 2017; Kiritsi and Nyström, 2018). PGRN has multiple physiological functions and is involved in many types of disease processes, including autoimmune disorders (Jian et al., 2018; Yu et al., 2018), cancer (Ding et al., 2018; Li et al., 2018), and neurodegenerative diseases (Mao et al., 2017; Paushter et al., 2018). The mRNA expression of PGRN increases significantly after injury while PGRN stimulates proliferation and migration of dermal fibroblasts and endothelial cells in vitro (He et al., 2003). Thus, we

hypothesized that PGRN could affect the fibrosis process of wound healing.

We found PGRN mRNA and protein expressions increased after insult and remained above that of intact skin through day 20. PGRN did not express in intact skin but highly expressed in the recruited MNCs and FBCs. These indicate a role for PGRN in inflammation and fibrosis processes of the wound response. Previous studies have authenticated that PGRN inhibits inflammation. One of the mechanisms is that PGRN binds both TNF receptor I and II to block the TNF-α-mediated inflammatory signaling pathway (Alquézar et al., 2016; Wei et al., 2016).

However, there is a paucity of studies mentioning the relationship between PGRN and fibrosis so far. Kanako Yasui et al. reported an increased expression of PGRN in the skin of amyotrophic lateral sclerosis patients, which has markedly decreased diameter of collagen fibrils, decreased amount of collagen, increased solubility of collagen and decreased collagen IV (Yasui et al., 2011). Yilmaz et al. found that PGRN expression in patients' serum with non-alcoholic fatty liver was higher and maybe related to the degree of hepatic fibrosis (Yilmaz et al., 2011). These indicate that PGRN plays an important role in fibrosis. In the present study, reduction of PGRN aggregated the degree of fibrosis. Not only the number of fibroblasts increased rapidly and peaked at day 8 in advance, but also the fibric areas were lager, the skins were thicker and the expression of Col I increased after PGRN knockdown. Thus, we confirm

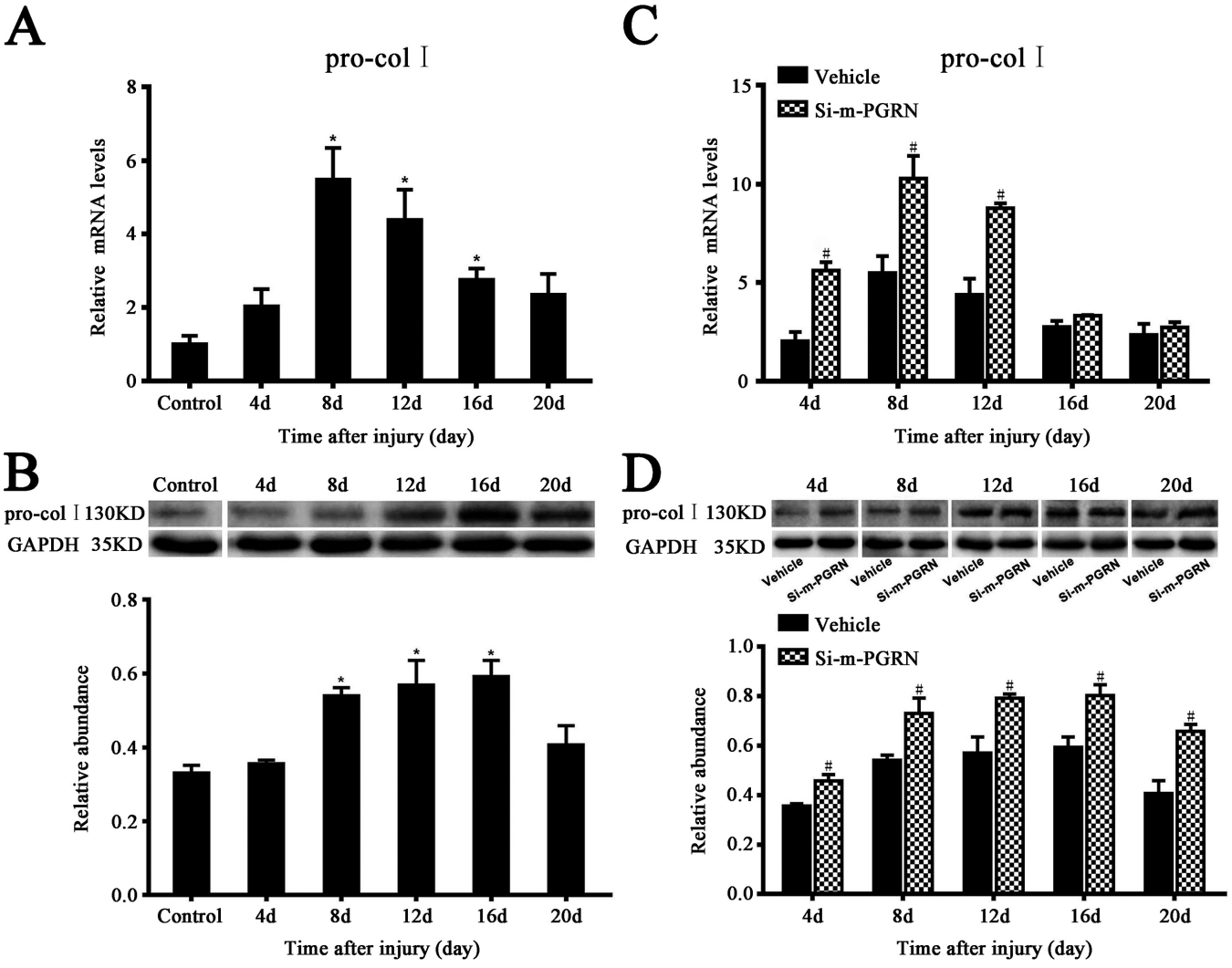

Fig. 3. Reduction of PGRN increased collagen deposition. **A.** pro-col I mRNA expression levels in the vehicle group and the control group were analyzed by RT-qPCR and normalized to β-actin. **B.** Representative Western blot analysis for pro-col I in the vehicle group and the control group. **C.** The effects of si-m-PGRN on the mRNA levels of pro-col I were analyzed by RT-qPCR and normalized to β-actin. **D.** Representative Western blot analysis for pro-col I protein levels after PGRN knockdown. All values are expressed as the mean ± standard deviation (n=5). *P<0.05, compared with the control group. #P<0.05, compared with the vehicle group.

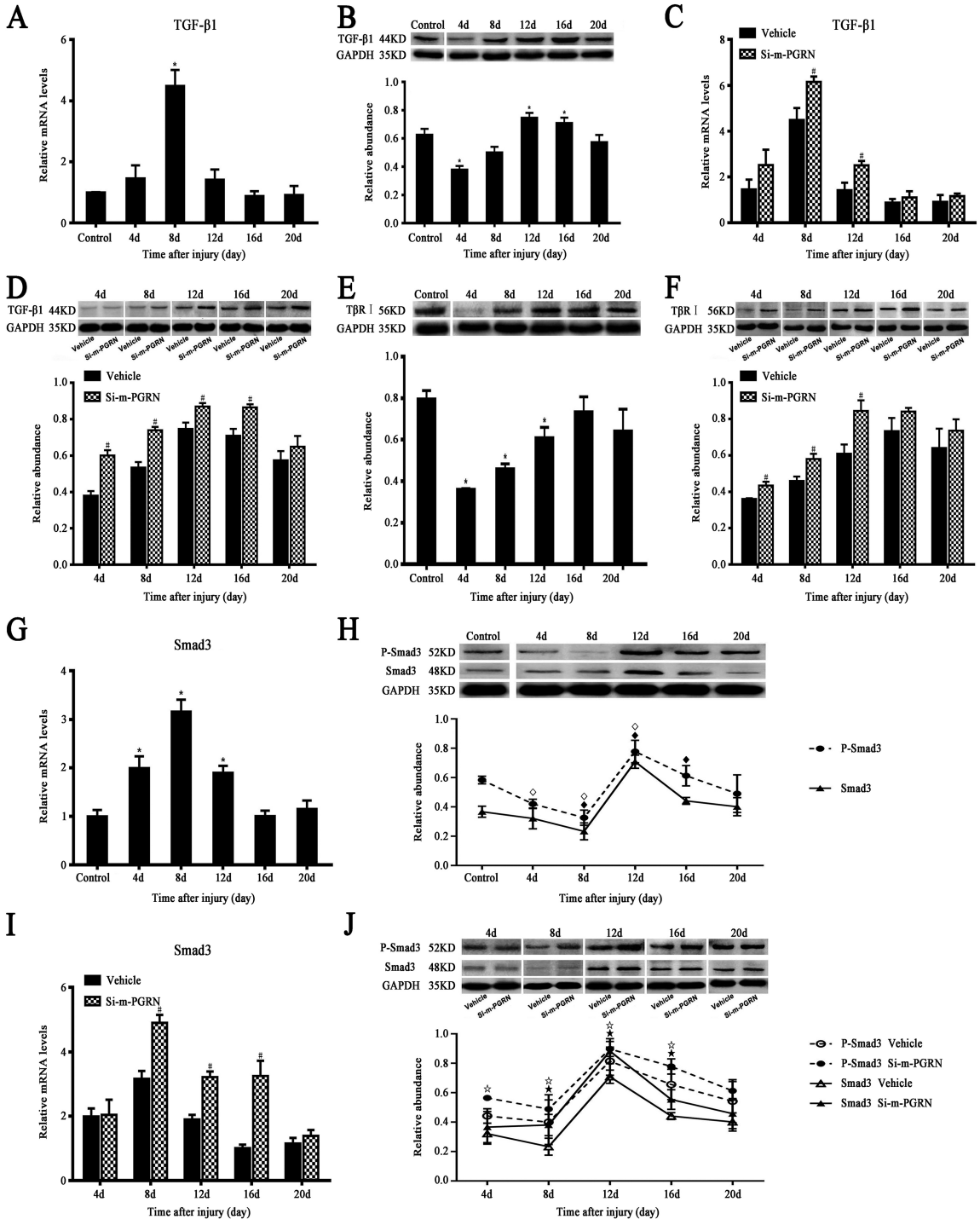

Fig. 4 Reduction of PGRN regulated TGF-β/Smad signaling pathway. **A.** TGF-β1 mRNA expression levels in the vehicle group and the control group were analyzed by RT-qPCR and normalized to β-actin. **B.** Representative Western blot analysis for TGF-β1 in the vehicle group and the control group. **C.** The effects of si-m-PGRN on the mRNA levels of TGF-β1 were analyzed by RT-qPCR and normalized to β-actin. **D.** Representative Western blot analysis for TGF-β1 protein levels after the down-regulation of PGRN by si-m-PGRN. **E.** Representative Western blot analysis for TβRI in intact and post-injury skin. **F.** Representative Western blot analysis for TβRI protein levels after PGRN knockdown by siRNA. **G.** Smad3 mRNA expression levels after injury were analysed by RT-qPCR and normalized to β-actin. **H.** Representative Western blot analysis for P-Smad3 and Smad3 in the vehicle group and the control group. **I.** Smad3 mRNA expression levels in the vehicle group and the si-m-PGRN group were analysed by RT-qPCR and normalized to β-actin. **J.** The effects of si-m-PGRN on the expression of P-Smad3 and Smad3 in post-injury skin were detected by Western blot. All values are expressed as the mean ± standard deviation (n=5). *P<0.05, compared with the control group. #P<0.05, compared with the vehicle group. ◇P<0.05, compared with the control group (P-Smad3). ◆P<0.05, compared with the control group (Smad3). ☆P<0.05, compared with the vehicle group (P-Smad3). ★P<0.05, compared with the vehicle group (Smad3).

that PGRN may reverse-regulate fibric process.

As is well known, TGF-β1 has a particular importance in the fibrosis process of skin wound healing (Makboul et al., 2014). During wound healing after injury, platelets are an initial source of TGF-β, but wound fibroblasts may be capable of autoamplification of the initial response to injury by increasing TGF-β mRNA and protein after activation (Tredget et al., 2000). TGF-β1 inhibits proliferation of keratinocytes, whereas it stimulates proliferation of dermal fibroblasts (Ghosh, 2002; Yu et al., 2009; Cho et al., 2010). Our results showed that the protein expression of TGF-β1 was highest on day 12 after surgery, so was the number of fibroblasts. In systemic sclerosis, TGF-β is significantly increased in bleomycin-induced skin fibrosis, and the phosphorylation of its downstream Smad is also enhanced. Dysregulated TGF-β/Smad2/3 signaling is thought to be crucial in the upregulation of type I collagen (Mori et al., 2003). In this study, the expression of TGF-β1, TβRI and P-Smad3 was up-regulated, and the expression level was closely related to the post injury interval, which is consistent with our previous results (Li et al., 2016). Furthermore, Tanaka et al. found that PGRN deficiency increased TGF-β1 production and Smad3 in microglia and astrocytes, and then aggravated the extent of glial scars (Tanaka et al., 2013). Our results have shown that TGF-β1, TβRI Smad3 and P-Smad3 increased in the PGRN knockdown group, indicating that reduction of PGRN up-regulates the TGF-β/Smad3 signaling pathway. We can infer that PGRN can regulate fibrosis by affecting the expression of TGF-β1, but confirmation still needs further studies.

Taken together, our present study demonstrates that PGRN plays a crucial role in the fibrosis process of cutaneous wound healing, which may be via the TGF-β1/Smad3 pathway.

Acknowledgements. This study was supported by the Natural Science Foundation of the Jiangsu Higher Education Institutions of China (16KJB340002), Jiangsu Overseas Visiting Scholar Program for University Prominent Young & Middle-aged Teachers and Presidents (2017), Jiangsu province postgraduate training innovation project (KYCX17-1730), Xuzhou Science and Technology Plan Project (KC15SM047), Natural Guidance Project of Colleges in Jiangsu (15KJD180003), and Xuzhou Medical University Scientific Research Fund for Talents (D2016004 and D2016005).

References

Alquézar C., de la Encarnación A., Moreno F., López de Munain A. and Martín-Requero Á. (2016). Progranulin deficiency induces overactivation of WNT5A expression via TNF-α/NF-κB pathway in peripheral cells from frontotemporal dementia-linked granulin mutation carriers. J. Psychiatry Neurosci. 41, 225-239.

Cho J.W., Kang M.C. and Lee K.S. (2010). TGF-β1-treated ADSCs-CM promotes expression of type I collagen and MMP-1, migration of human skin fibroblasts, and wound healing in vitro and in vivo. Int. J. Mol Med. 26, 901-906.

Ding D., Li C., Zhao T., Li D., Yang L. and Zhang B. (2018). LncRNA H19/miR-29b-3p/PGRN Axis promoted epithelial-mesenchymal transition of colorectal cancer cells by acting on Wnt signaling. Mol. Cells. 41, 423-435.

Eming S.A., Wynn T.A. and Martin P. (2017). Inflammation and metabolism in tissue repair and regeneration. Science 356, 1026-1030.

Ghosh A.K. (2002). Factors involved in the regulation of type I collagen gene expression: implication in fibrosis. Exp. Biol. Med. (Maywood). 227, 301-314.

Gurtner G.C., Werner S., Barrandon Y. and Longaker M.T. (2008). Wound repair and regeneration. Nature 453, 314-321.

He Z., Ong C.H., Halper J. and Bateman A. (2003). Progranulin is a mediator of the wound response. Nat. Med. 9, 225-229.

Jian J., Li G., Hettinghouse A. and Liu C. (2018). Progranulin: A key player in autoimmune diseases. Cytokine 101, 48-55.

Kiritsi D. and Nyström A. (2018). The role of TGFβ in wound healing pathologies. Mech. Ageing Dev. 172, 51-58.

Li S.S., Wang L.L., Liu M., Jiang S.K., Zhang M., Tian Z.L., Wang M., Li J.Y., Zhao R. and Guan D.W. (2016). Cannabinoid CB2 receptors are involved in the regulation of fibrogenesis during skin wound repair in mice. Mol. Med. Rep. 13, 3441-3450.

Li G., Dong T., Yang D., Gao A., Luo J., Yang H. and Wang L. (2018). Progranulin promotes lymphangiogenesis through VEGF-C and is an independent risk factor in human esophageal cancers. Hum. Pathol. 75, 116-124.

Makboul M., Makboul R., Abdelhafez A.H., Hassan S.S. and Youssif S.M. (2014). Evaluation of the effect of fractional CO2 laser on histopathological picture and TGF-β1 expression in hypertrophic scar. J. Cosmet. Dermatol. 13, 169-179.

Mao Q., Wang D., Li Y., Kohler M., Wilson J., Parton Z., Shmaltsuyeva B., Gursel D., Rademakers R., Weintraub S., Mesulam M.M., Xia H. and Bigio E.H. (2017). Disease and region specificity of granulin immunopositivities in Alzheimer disease and frontotemporal lobar degeneration. J. Neuropathol. Exp. Neurol. 76, 957-968.

Mori Y., Chen S.J. and Varga J. (2003). Expression and regulation of intracellular SMAD signaling in scleroderma skin fibroblasts. Arthritis Rheum.48, 1964-1978.

Paushter D.H., Du H., Feng T. and Hu F. (2018). The lysosomal function of progranulin, a guardian against neurodegeneration. Acta Neuropathol. 136, 1-17.

Seo G.Y., Lim Y., Koh D., Huh J.S., Hyun C., Kim Y.M. and Cho M. (2017). TMF and glycitin act synergistically on keratinocytes and fibroblasts to promote wound healing and anti-scarring activity. Exp. Mol. Med. 49, e302.

Tanaka Y., Matsuwaki T., Yamanouchi K. and Nishihara M. (2013). Exacerbated inflammatory responses related to activated microglia after traumatic brain injury in progranulin-deficient mice. Neuroscience 231, 49-60.

Tredget E.E., Wang R., Shen Q., Scott P.G. and Ghahary A. (2000). Transforming growth factor-beta mRNA and protein in hypertrophic scar tissues and fibroblasts: antagonism by IFN-alpha and IFN-gamma in vitro and in vivo. J. Interferon Cytokine Res. 20, 143-151.

Wang L.L., Zhao R., Li J.Y., Li S.S., Liu M., Wang M., Zhang M.Z., Dong W.W., Jiang S.K., Zhang M., Tian Z.L., Liu C.S. and Guan D.W. (2016). Pharmacological activation of cannabinoid 2 receptor attenuates inflammation, fibrogenesis, and promotes re-epithelialization during skin wound healing. Eur. J. Pharmacol. 786, 128-136.

Wei J., Hettinghouse A. and Liu C. (2016). The role of progranulin in arthritis. Ann. NY Acad. Sci. 1383, 5-20.

Yasui K., Oketa Y., Higashida K., Fukazawa H. and Ono S. (2011). Increased progranulin in the skin of amyotrophic lateral sclerosis: an immunohistochemical study. J. Neurol. Sci. 309, 110-114.

Yilmaz Y., Eren F., Yonal O., Polat Z., Bacha M., Kurt R., Ozturk O. and Avsar E. (2011). Serum progranulin as an independent marker of liver fibrosis in patients with biopsy-proven nonalcoholic fatty liver disease. Dis. Markers 31, 205-210.

Yu H., Mrowietz U. and Seifert O. (2009). Downregulation of SMAD2, 4 and 6 mRNA and TGFbeta receptor I mRNA in lesional and non-lesional psoriatic skin. Acta Derm. Venereol. 89, 351-356.

Yu Y., Shi Y., Zuo X., Feng Q., Hou Y., Tang W., Lu Y., Yi F., Hou M., Yu Y. and Peng J. (2018). Progranulin facilitates the increase of platelet count in immune thrombocytopenia. Thromb. Res. 164, 24-31.

Accepted December 18, 2018